



HAL
open science

Implementation of an advanced photooxidation process to intensify pharmaceuticals removal by a membrane bioreactor

Brice Reoyo-Prats, Mouldi Hammadi, Suveechard Kim Lai, Vincent Goetz,
Carole Calas-Blanchard, Claire Joannis-cassan, Gaël Plantard

► To cite this version:

Brice Reoyo-Prats, Mouldi Hammadi, Suveechard Kim Lai, Vincent Goetz, Carole Calas-Blanchard, et al.. Implementation of an advanced photooxidation process to intensify pharmaceuticals removal by a membrane bioreactor. *Chemical Engineering and Processing: Process Intensification*, 2023, 191, pp.109460. 10.1016/j.cep.2023.109460 . hal-04200867

HAL Id: hal-04200867

<https://cnrs.hal.science/hal-04200867>

Submitted on 8 Sep 2023

HAL is a multi-disciplinary open access archive for the deposit and dissemination of scientific research documents, whether they are published or not. The documents may come from teaching and research institutions in France or abroad, or from public or private research centers.

L'archive ouverte pluridisciplinaire **HAL**, est destinée au dépôt et à la diffusion de documents scientifiques de niveau recherche, publiés ou non, émanant des établissements d'enseignement et de recherche français ou étrangers, des laboratoires publics ou privés.

1 Implementation of an advanced photooxidation process 2 to intensify pharmaceuticals removal by a membrane 3 bioreactor

4
5 REOYO-PRATS Brice^a ; HAMMADI Mouldi^a ; KIM LAI Suveechard^b ; GOETZ Vincent^a ;
6 CALAS-BLANCHARD Carole^c ; JOANNIS-CASSAN Claire^b and PLANTARD Gaël^{a,*}

7
8 ^aPROMES-CNRS UPR 8521, PROcess Material and Solar Energy, Rambla de la Thermodynamique 66100
9 Perpignan, France.

10 ^bLaboratoire de Génie Chimique, Université de Toulouse, CNRS, INPT, UPS, Toulouse, France.

11 ^cCentre de Phytopharmacie, CNRS UMR 5054, Université de Perpignan, 52 Avenue de Villeneuve, 66860
12 Perpignan, France.

13 * Corresponding author: plantard@univ-perp.fr

16 Abstract

17 Removal of pharmaceuticals from wastewaters is of particular importance nowadays. If biodegradable
18 molecules can be nearly totally eliminated by biological treatments such as membrane bioreactor (MBR),
19 many pharmaceuticals are recalcitrant. To improve the removal of these micropollutants, an advanced
20 oxidation process (AOP), based on TiO₂ photocatalyst, has been implemented on a recirculation loop on a
21 15-L MBR operated with a sludge retention time (SRT) of 30d and a hydraulic retention time (HRT) of 48h.
22 This innovative process did not negatively impact the bacterial community of the MBR which maintained
23 same a Total Suspended Solids (TSS) concentration of 5g.L⁻¹ and a high carbon removal yield (> 92 %). For
24 different flux densities tested (4, 17 and 40 W.m⁻²), similar degradation efficiency was observed for two
25 pharmaceuticals: ibuprofen (IBU) and carbamazepine (CBZ). Thus, a flux density of 4 W.m⁻² was selected
26 for the coupling. This configuration intensified the degradation of CBZ by a factor 10 (up to 28 % removal)
27 in comparison with the MBR alone and the removal of IBU was maintained close to 99 %.

28
29 Keywords: pharmaceuticals, wastewater, photooxidation, membrane bioreactor, intensification.

30

31

32 **1. Introduction**

33 The Water Framework Directive [1] provides for policy measures to protect the environment and human
34 health against risks tied to toxic pollution by setting objectives that aim to reduce or even eliminate
35 discharges of specific substances and to achieve good ecological status. It thus makes water and sewage
36 management and reuse a strategic economic, social and above all environmental challenge [2]. The issue
37 is acutely focused on organic pollutants and pharmaceutical compounds [3]. With improved analytical
38 techniques and lower limits of quantification, pollutants have now been detected in natural waters at
39 concentrations between ng.L^{-1} and $\mu\text{g.L}^{-1}$ [4–6]. The vast majority of these pollutants comes from
40 wastewater treatment plant effluents, but some also come from hospital effluents [7,8]. Many of these
41 substances readily is subject to biodegradation biodegrade and can therefore be degraded by biological-
42 process treatment or by long periods in the environment. This is the case for many analgesics and some
43 antibiotics [5,9,10]. However, there is another category of substances called persistent organic pollutants
44 (POPs) that are more recalcitrant to conventional treatments. POPs cover a wide spectrum of drugs
45 ranging from anti-inflammatories and antidepressants to antibiotics and beta-blockers [5,9], but all are
46 suspected to be carcinogenic or endocrine disruptors, which makes them the focal challenge of pollution
47 management measures.

48 Wastewater treatment plants (WWTP) based on biological processes (typically activated sludge) are still
49 not fully effective in degrading organic micropollutants, especially POPs. The capacity of a biological
50 treatment depends on both the properties of the molecules (chemical structure, sorption capacity,
51 hydrophobicity, and son) and on the operational WWTP biological process parameters applied (hydraulic
52 residence time, sludge residence time, etc.). Some pharmaceutical products, such as diclofenac or
53 carbamazepine, are only partially eliminated with efficiencies below 40% while others, like ibuprofen, are
54 relatively well eliminated (> 70%) [11,12]. Intensifying biological processes with technologies such as
55 membrane bioreactor (MBR) has demonstrated better removal of most pharmaceuticals than activated
56 sludge but still fails to completely remove all micropollutants [13,14].

57 In this context, many organic substances that are toxic or resistant to biological treatment continually get
58 released into water bodies, soils, and other natural habitats [4]. A promising way forward is to complete
59 this biological process with an advanced technology based on chemical oxidation. These advanced
60 oxidation processes (AOPs) are widely recognized as very effective treatments for recalcitrant wastewater
61 [15,16]. They are environmentally-friendly processes that hold the advantage of non-selectively

62 eliminating contaminant loads. Most AOPs are aqueous-phase oxidation processes based on producing
63 hydroxyl radicals, the second strongest oxidant after fluorine, which have enough oxidizing power to
64 destroy practically all types of organic contaminants [17,18]. AOPs generate large amounts of hydroxyl
65 radicals under specific operating conditions. Studies have demonstrated the effectiveness of both
66 advanced oxidation processes and solar photocatalytic oxidation [15,19].

67 Thus, a combination of biological and AOP processes could improve the all-round removal of
68 micropollutants to achieve the abatement performance levels required under future regulatory
69 constraints [20,21]. In the literature, several studies have tested the association of a biological process
70 with an AOP to eliminate organic pollutants. In all these studies, the two processes are associated in series
71 (sequentially) in two different configurations. The first configuration consists in positioning the oxidation
72 process upstream as a pre-treatment [22,23]. The utility lies in the oxidation of biorecalcitrant substances,
73 thus making the effluent biodegradable. The disadvantage is that it yields a complex effluent that contains
74 pollutants at sometimes high concentrations along with suspended matter. This complex matrix could
75 inhibit the specific degradation of the pollutants targeted by this treatment by increasing the competition
76 between the substances. Increasing the quantity of total matter to be oxidized renders the treatment
77 capacity of the oxidation process inadequate or even ineffective. It also negates the value of non-selective
78 degradation, since in this case all pollutants—including biodegradables—will get oxidized during this step.

79 The second configuration for coupling the two processes in series consists in positioning the AOP
80 downstream of the biological process as a tertiary or quaternary treatment [21,24,25]. The objective here
81 is to improve the biological treatment by oxidizing the substances that have been partially or not degraded.
82 The challenge with this association is to degrade molecules that are at very low concentrations in large
83 volumes of water and ensure that they are totally mineralized and thus not released into the environment.

84 The innovative association proposed in this paper consists of a compromise between these two modes of
85 association in a way that exploits the advantages of each. The biological process is a MBR because of its
86 high pharmaceutical removal performance and its suspended solids-free outlet. The AOP is based on
87 titanium dioxide (TiO₂) photocatalysis which non-selectively but very efficiently degrades organic
88 pollutants such as pharmaceuticals. The concept is based on coupling the two processes, where the AOP
89 is not staged in series with the MBR but in a recirculation loop on the MBR itself. In this configuration, the
90 final objective of the AOP is not to fully mineralize the POPs leaving the MBR but to partially transform
91 them into biodegradable substances that are then eliminated when they are re-streamed back into the
92 MBR [26]. The purpose of this combined technological configuration is to obtain a stronger synergistic
93 effect than the simple sequential implementation of the two processes (MBR + AOP).

94 To evaluate the performance of the coupled reactors, the progress of two pharmaceutical molecules were
95 tracked through the process: ibuprofen (IBU) and carbamazepine (CBZ). These two molecules were chosen
96 as they are both widely encountered in WWTPs and in freshwaters [8,27,28] but have different toxicity
97 profiles and different biodegradability levels [29,30]. Ibuprofen is highly biodegradable whereas
98 carbamazepine is biorecalcitrant. Many studies on titanium dioxide photocatalysis for pharmaceutical
99 wastewater removal have employed these same molecules for the same reasons [31].
100 The aim of this study was to prove the feasibility and utility of this mode of process association by
101 investigating whether recirculating the effluent in an oxidation process increases MBR efficiency. For that
102 purpose, pharmaceutical removal rates in a 15-L MBR alone versus a MBR coupled with a photooxidation
103 process were compared. The MBR was operated with a sludge retention time (SRT) of 30d and a hydraulic
104 retention time of 48h. The photo-oxidation process was tested at several flux densities.

105 **2. Material and Methods**

106 **2.1. Standardized Synthetic effluent**

107 Carbamazepine (CBZ) and ibuprofen (IBU) were purchased from Sigma–Aldrich MO (100% purity; Sigma-
108 Aldrich, MO). A concentrated solution was prepared weekly in tap water at a concentration of 50 $\mu\text{g}\cdot\text{L}^{-1}$ for
109 CBZ and 400 $\mu\text{g}\cdot\text{L}^{-1}$ for IBU.

110 The concentrated synthetic wastewater was composed of peptone (4800 $\text{mg}\cdot\text{L}^{-1}$), meat extract (3300 $\text{mg}\cdot\text{L}^{-1}$),
111 K_2HPO_4 (210 $\text{mg}\cdot\text{L}^{-1}$), NaCl (52.5 $\text{mg}\cdot\text{L}^{-1}$), CaCl_2 (120 $\text{mg}\cdot\text{L}^{-1}$), MgSO_4 (60 $\text{mg}\cdot\text{L}^{-1}$), NH_4Cl (750 $\text{mg}\cdot\text{L}^{-1}$) and
112 NaOAc (600 $\text{mg}\cdot\text{L}^{-1}$). These substances have been diluted in tap water, corresponding to a chemical
113 oxygen demand (COD) of 1000 $\text{mg}\cdot\text{L}^{-1}$, a total N (TN) content of 120 $\text{mg}\cdot\text{L}^{-1}$ and a total P (TP)
114 content of 10 $\text{mg}\cdot\text{L}^{-1}$. pH was maintained at 7.2. The composition of this standardized synthetic
115 effluent based on OECD guidelines which is characteristic of wastewater from wastewater
116 treatment plants, is commonly used in the literature [32]. A standardized synthetic effluent makes
117 it possible to carry out a series of experiments over a long period of time with reproducible feeding
118 conditions and to be able to compare the performance of the system from one experiment to
119 another.

120

121 **2.2. Experimental set-ups**

122 **2.2.1. Membrane bioreactor**

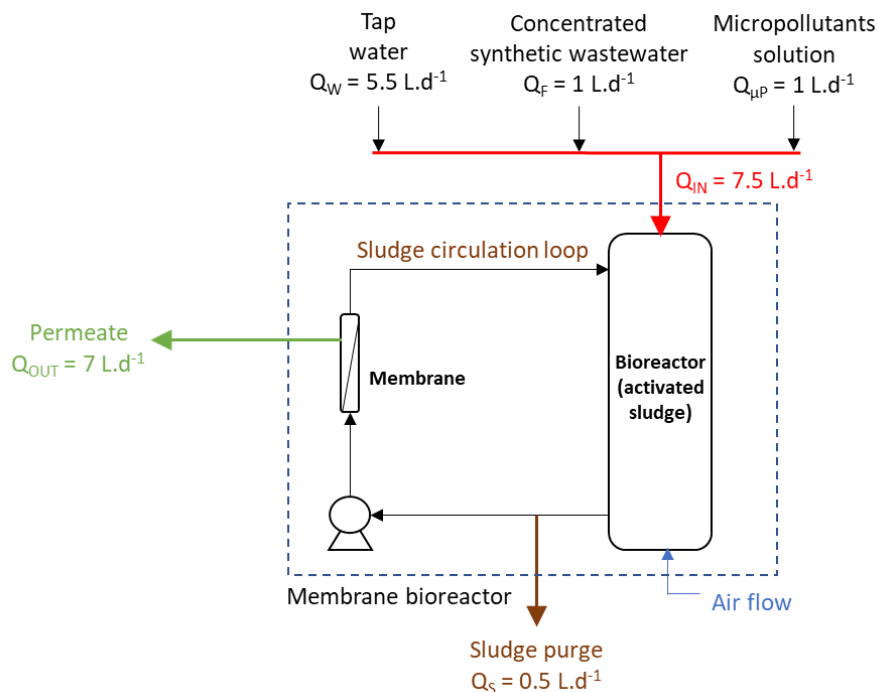
123 A 15 L MBR equipped with a Rushton turbine (200 rpm) was operated at a hydraulic retention time
124 $\text{HRT}_{\text{MBRalone}} = 48$ h and a sludge retention time (SRT) of 30 d (**Fig. 1**). At the initial start-time, the MBR was

125 filled with activated sludge sourced from a real WWTP (Perpignan, France) with a total suspended solids
126 (TSS) concentration of 2.5 g.L^{-1} . A tubular ceramic membrane (Membralox®, Pall Exekia, France) with
127 surface area of 0.0055 m^2 and pore size of $0.2 \mu\text{m}$ was positioned in an external module. Tangential velocity
128 in the membrane was set at 4.5 m.s^{-1} . Probes were used to monitor temperature, dissolved oxygen and
129 pH. pH was adjusted to 7 by adding NaOH at the beginning. Cycles of 5 min aeration (dissolved oxygen of
130 $6 \text{ mg}_{\text{O}_2}.\text{L}^{-1}$) / 40 min without aeration were used to create aerobic/anoxic conditions for the nitrification
131 and denitrification steps [33].

132 The MBR was continuously fed at a flow rate of $Q_{\text{IN}} = 7.5 \text{ L.d}^{-1}$ (Fig. 1). This inflow was composed of 1 L.d^{-1}
133 of concentrated synthetic solution, 1 L.d^{-1} of concentrated micropollutant solution, and 5.5 L.d^{-1} of tap
134 water. Consequently, composition at the MBR infeed was: 1000 mg.L^{-1} chemical oxygen demand (COD),
135 120 mg.L^{-1} total nitrogen (TN) and 10 mg.L^{-1} total phosphorus (TP). Inlet concentrations of micropollutant
136 were $7 \mu\text{g.L}^{-1}$ CBZ and $53 \mu\text{g.L}^{-1}$ IBU. These concentrations were chosen to be representative of real
137 concentrations measured in thousands of WWTP in the EU [34] and across the world [14].

138 After a 70 d adaptation phase, the MBR was considered to be in a steady state (TSS and outlet
139 concentrations were constant). Every two or three days, 20 mL samples of the feed solution and permeate
140 were taken at end of the anoxic phase and frozen at $-20 \text{ }^\circ\text{C}$ until analysis to determine COD, TN, NH_4^+ , NO_2^-
141 and NO_3^- concentrations. Samples of sludge (evenly taken away at a flow rate of $Q_S = 0.5 \text{ L.d}^{-1}$) were also
142 collected at regular intervals to measure TSS and volatile suspended solids (VSS).

143



144

145
146
147
148
149
150
151
152
153
154
155
156
157
158
159
160
161
162
163
164
165
166
167
168
169
170
171
172
173
174
175
176

Figure 1: Synoptic of the experimental set up of the membrane bioreactor.

2.2.2. Photoreactor pilot

The lab-scale photoreactor (**Fig. 2**) was composed of a single closed 2 L flat-panel (25 x 45 x 2 cm) parallelepiped-shaped reactor with a stainless-steel base and a UV-transparent (91 % UV transmission) PMMA plate covering the front. Irradiance source was an artificial LED UV panel of the same surface area as the tank to deliver uniform irradiance. This LED UV panel was set 2 cm from the PMMA surface. Irradiance was delivered in a very narrow spectrum centered around 365 nm. After calibration with a MU-200 UV sensor (Apogee Instrument, Logan, UT, USA), radiant flux density at the reactor surface was controllable and adjustable between 5 and 85 W.m⁻². As the solar UV flux density varies from 0-50 W.m⁻², three flux densities representative of the solar irradiation range were selected: 4, 17 and 40 W.m⁻² [17].

Titanium dioxide (TiO₂) was chosen as it is one of the most attractive catalysts for environmental remediation [35], used in its photosphere form, i.e. 45 μm (range: 5 μm–85 μm) TiO₂-coated glass microspheres. The advantage of this form is that it floats (0.22 g.L⁻¹ density) and is therefore easier to separate from treated water. The optimal photocatalyst concentration corresponds to total absorption of the radiation inducing the fastest kinetics [36]. Preliminary tests (data not shown) run with varying photosphere concentrations concluded that a concentration of 5 g.L⁻¹ maximized the pollutant degradations kinetics. Fresh catalyst was used at the start of each experiment. The photospheres were homogenized in the water by pressurized airflow pumped into the tank bed via five holes evenly spaced across the width.

The photoreactor, filled with 2l of effluent, develops a light capture surface of 0.12 m². The pilot was used in continuous mode, driven for the inlet by a peristaltic pump (Watson Marlow 205U) at 7.5 L.d⁻¹ (HRT_{OX} = 6.4 h) for the micropollutant solution inflow (Q_{μP}). For the outlet, just overflow/water-levelling was used (Q_{OX}). To achieve the separation between the catalyst and treated water, i.e. avoid release into the sewer system and maintain its concentration in the photoreactor, we purpose-engineered a flotation system composed of a reverse funnel.

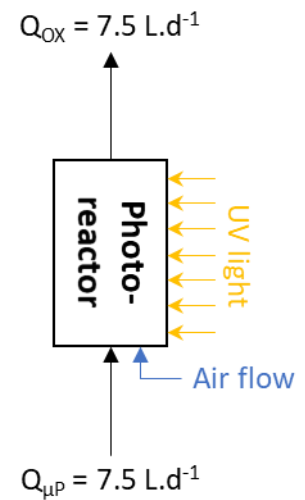


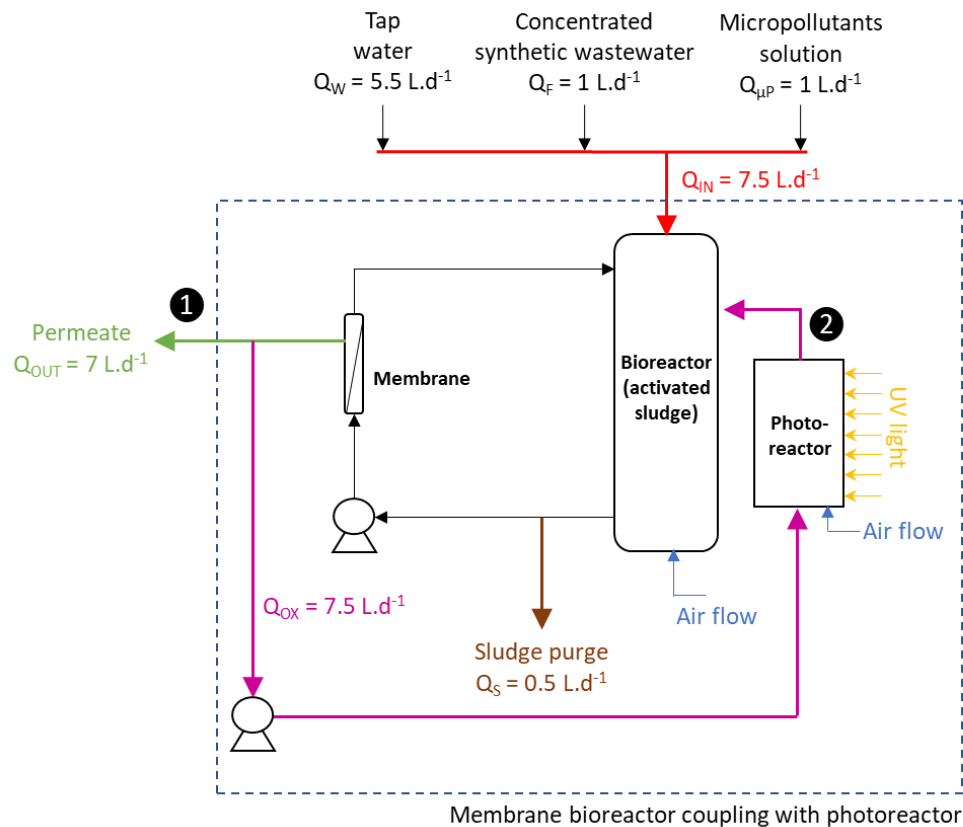
Figure 2: Synoptic of the experimental set up of the photoreactor.

177 **2.2.3. Coupling the membrane bioreactor with the photoreactor**

178 The MBR was first inoculated in the same way as presented in 2.2.1. After the adaptation phase, the
179 photoreactor was hydraulically connected (UV turned off) with the MBR by a recirculation loop at a flow
180 rate of 7.5 L.d⁻¹ via the same peristaltic pump (Watson Marlow 205U) (**Fig. 3**). The flows previously stated
181 for the MBR (Q_F , $Q_{\mu P}$, Q_S , Q_{OUT} , **Fig. 1**) and the photoreactor (Q_{OX} , **Fig. 2**) were kept the same, leading to the
182 same flows for the final coupled system (**Fig. 3**). In this configuration, the HRT of the MBR ($HRT_{MBRcoupled}$)
183 was 24 h with a global flow of 15 L.d⁻¹.

184 After 8 days of running without oxidation, the UV lamp of the photoreactor was turned on. The same
185 sampling procedure as for the MBR was repeated for global parameter measurements (COD, TN, NH_4^+ ,
186 NO_2^- , NO_3^- , TSS, VSS).

187



188
189 **Figure 3:** Synoptic of the coupling of the membrane bioreactor with the photoreactor. Numbers in black discs are the
190 sampling points used to follow the pharmaceuticals degradation.

191

192 **2.3. Analytical methods**

193 **2.3.1. Sludge characterization**

194 The TSS and VSS contents of the activated sludge were measured according to standard methods 2540D
195 and 2540E [37].

196

197 2.3.2. Chemical characterization of the wastewater

198 COD, TN, NH₄-N, NO₂-N, NO₃-N, and TP concentrations were determined using to HACH Kits (LCK tubes)
199 with a HT200S thermostat (HACH) and a DR3900 spectrophotometer (HACH, Loveland, CO, USA).

200

201 2.3.3. Pharmaceutical compounds analysis

202 When the reactors were independent, samples were taken at the outlet (Q_{OUT}) of both the MBR (**Fig. 1**)
203 and the photoreactor (**Fig. 2**). When the reactors were coupled together, samples were taken at position
204 ❶ at the outlet of the MBR and position ❷ at the outlet of the photoreactor (**Fig. 3**). Three samples were
205 taken at steady state on 3 different days.

206 A volume of 150 mL was sampled then filtered through a 0.4 μm pore-size hydrophilic filter and mixed
207 with thiosulfate before being frozen at -20°C for storage pending dispatch to the COFRAC-accredited Carso
208 laboratory (France) for analysis. Concentrations were monitored at the lab by liquid chromatography–
209 tandem mass spectrometry (LC-MS/MS). Limits of quantification were 5 ng.L⁻¹ for CBZ and 100 ng.L⁻¹ for
210 IBU. All analyses were done in triplicate, and all results are average of the triplicate measures.

211

212 3. Results and Discussion

213 3.1. Carbon, nitrogen and phosphorus removal performances

214 As the main function of the MBR is to remove COD, TN and TP, the all-round performances of the MBR
215 were investigated with the photoreactor configured in coupled mode with the UV light turned off and then
216 turned on (inducing the photocatalysis process) as described in section 2.2.3.

217 The apparent removal efficiencies (E) of the MBR were calculated as follows:

$$218 E = \frac{C_{IN} - C_{OUT}}{C_{IN}} \cdot 100 \quad eq.1$$

219 where C_{IN} and C_{OUT} are concentration of the target parameter (COD, TN or TP) at the inlet and outlet
220 (position ❶), respectively (**Fig.3**).

221

222 **Table 1:** Apparent removal efficiency (E) for COD, TN and TP in coupling MBR-photoreactor without and with
223 oxidation step at 8.5 W.m⁻²

Apparent removal (E %)	
With UV lamp OFF	With UV lamp ON

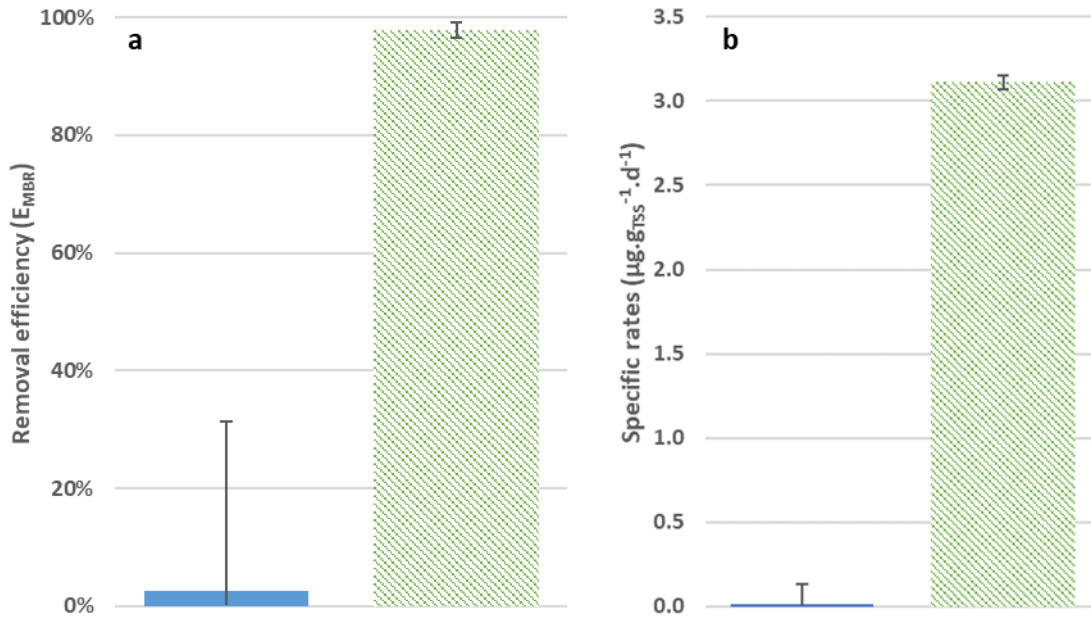
COD	92.3 ± 3.4	95.0 ± 0.7
TN	38.6 ± 15.5	56.8 ± 5.9
TP	25.3 ± 14.6	41.4 ± 25.4

224
 225 Mean removal of COD, TN and TP measured at steady state is shown in **Table 1**. Coupling the oxidation
 226 step with the MBR had no significant impact on COD and TN removal. For TP, the standard deviations were
 227 high due to some variations observed at the MBR outlet, making it is difficult to reach a firm conclusion on
 228 this parameter. The fact that these all-round performances were not negatively impacted by recirculating
 229 oxidized permeate into the MBR means that the photooxidation process had not impacted the microbial
 230 community for the duration of the oxidation step (20 days). It could be concluded that no toxic by-products
 231 were formed in the oxidative conditions tested, as even though the duration of this experiment was
 232 relatively short, there was no decrease in COD, TN and TP removal under any of the other oxidative
 233 conditions tested in this study. This result lays the foundations to implementing the innovative process
 234 proposed in this paper as a way to improve micropollutant removal.

235 **3.2. Removal of pharmaceuticals in the membrane bioreactor alone**

236 The MBR was first run independently in continuous mode at a flow of 7.5 L.d⁻¹ and an inlet concentration
 237 of 7 µg.L⁻¹ CBZ and 53 µg.L⁻¹ IBU to give a baseline reference (**Fig 1.**). The goal was to determine its removal
 238 efficiencies for the two pharmaceuticals in order to compare them with the removal efficiency of the
 239 coupled system.

240 At steady state, the average of triplicate outlet concentration measurements was 6.8 (±2.0) µg.L⁻¹ for CBZ
 241 and 1.1 (±0.7) µg.L⁻¹ for IBU. Comparison of these final concentrations with the initial 'reference'
 242 concentrations finds that the MBR did not degrade CBZ but was able to degrade IBU by a factor of 50.
 243 To overcome the difference in initial concentrations between CBZ (7 µg.L⁻¹) and IBU (53 µg.L⁻¹), the
 244 apparent removal efficiencies (E_{MBR}) of the MBR were recalculated using *Eq.1* and considering C_{IN} as the
 245 inlet micropollutant concentration and C_{OUT} as the outlet micropollutant concentration (see **Fig. 1**).
 246



247
 248 **Figure 4:** carbamazepine [plain blue] and ibuprofen [green zebras], removal efficiencies (left) and specific rates (right)
 249 by the membrane bioreactor alone.

250
 251 The MBR alone thus had a removal efficiency of no more than 3 % (±29) for CBZ but 98 % (±1) for IBU
 252 (**Fig. 4a**). These figures are in the range of value reported in the literature that finds CBZ to be
 253 biorecalcitrant (E between -42 % and 51 %) and IBU to be readily biodegradable (E between 73 % and
 254 100 %) [14,38,39].

255 To push the analysis further, the specific biodegradation rate (r_{MBR} , $\mu\text{g.g}_{TSS}^{-1}.\text{d}^{-1}$) and the first-order
 256 biodegradation rate constant (k_{biol} , $\text{L.g}_{TSS}^{-1}.\text{d}^{-1}$) were calculated. As sorption of both IBU and CBZ can be
 257 neglected (<5%), [40, 41], the specific biodegradation rate has been estimated in steady state as follows:

$$258 \quad r_{MBR} = \frac{Q_{IN} \cdot (C_{IN} - C_{OUT})}{V_{MBR} \cdot C_{TSS}} \quad eq.2$$

259 where C_{TSS} is sludge concentration (5 g.L^{-1}) and V_{MBR} is volume of MBR. With the same assumption of
 260 negligible sorption, the biodegradation rate constant was estimated as follows:

$$261 \quad k_{biol} = \frac{Q_{IN} \cdot (C_{IN} - C_{OUT})}{V_{MBR} \cdot C_{TSS} \cdot C_{OUT}} \quad eq.3$$

262 Comparison of the specific biodegradation rates of IBU and CBZ (**Fig. 4b**) shows that biodegradation was
 263 300 times faster for IBU than for CBZ ($3.11 \pm 0.04 \mu\text{g.g}_{TSS}^{-1}.\text{d}^{-1}$ for IBU vs. $0.01 \pm 0.12 \mu\text{g.g}_{TSS}^{-1}.\text{d}^{-1}$ for CBZ).
 264 This is mainly due to the biodegradability of the IBU which was very sensitive to microbial activity in the
 265 MBR and accentuated by the fact that the IBU was more concentrated in the feed effluent ($C_{IBU} = 53 \mu\text{g.L}^{-1}$)

266 ¹ vs $C_{CBZ} = 7 \mu\text{g.L}^{-1}$), whereas CBZ, due to its persistent nature, proved very resistant to biological
267 degradation.

268 This is confirmed by the values of the biodegradation rate constants, for which the ratio between IBU
269 ($2.76 \pm 0.03 \text{ L.g}_{\text{TSS}}^{-1}.\text{d}^{-1}$) and CBZ ($1.6 \times 10^{-3} \pm 0.24 \text{ L.g}_{\text{TSS}}^{-1}.\text{d}^{-1}$) was more than 1500. According to the
270 classification of [42], CBZ can be considered a 'hardly biodegradable' compound ($k_{\text{biol}} < 0.1 \text{ L.g}_{\text{TSS}}^{-1}.\text{d}^{-1}$) and
271 IBU as a 'highly biodegradable' compound ($1 < k_{\text{biol}} < 5 \text{ L.g}_{\text{TSS}}^{-1}.\text{d}^{-1}$). In the literature, depending on
272 operating conditions (HRT and SRT), k_{biol} in a MBR is always $< 0.1 \text{ L.g}_{\text{TSS}}^{-1}.\text{d}^{-1}$ for CBZ and in a range from 8
273 to $38 \text{ L.g}_{\text{TSS}}^{-1}.\text{d}^{-1}$ for IBU [40].

274

275 3.3. Removal of pharmaceuticals in the photoreactor alone

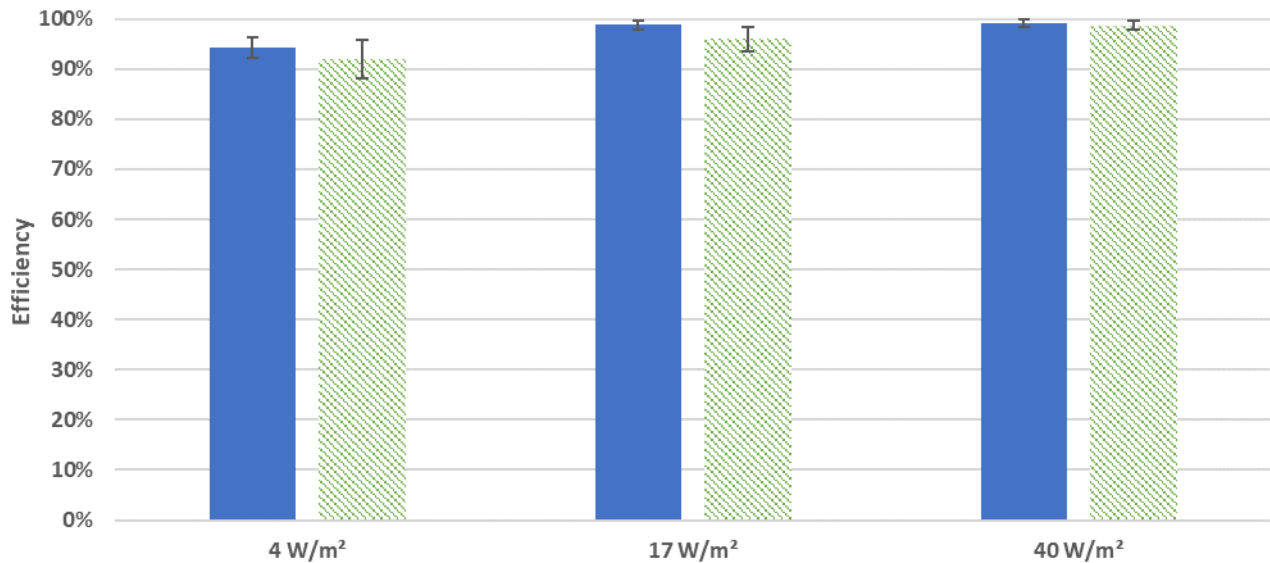
276 The photoreactor (Fig. 2) was operated in a continuous mode at a flow rate of 7.5 L.d^{-1} under three
277 different flux densities, i.e. 4 W.m^{-2} , 17 W.m^{-2} and 40 W.m^{-2} . This range of flux densities (4 to 40 W.m^{-2})
278 corresponds to the values of solar radiation during a standard day, and thus serves to test the utility of
279 using solar photooxidation processes for future real-world applications. As the work of Reoyo-Prats [44]
280 has shown that, over the range considered, the concentration level has a negligible influence on the rate
281 of degradation, these experiments used the concentrated solution of micropollutants ($50 \mu\text{g.L}^{-1}$ for CBZ
282 and $400 \mu\text{g.L}^{-1}$ for IBU) in order to obtain a better accuracy of the measurements.

283 Oxidation efficiency (E_{OX}) was calculated according to the following equation:

$$284 E_{\text{OX}} = \frac{C_{\mu\text{P}} - C_{\text{OX}}}{C_{\mu\text{P}}} \cdot 100 \quad \text{eq.4}$$

285 where $C_{\mu\text{P}}$ and C_{OX} are micropollutant concentration at the inlet and outlet of the photoreactor,
286 respectively (Fig.2).

287



288
 289 **Figure 5:** carbamazepine [plain blue] and ibuprofen [green zebras] removal efficiency by the photoreactor alone for
 290 different flux densities.

291
 292 **Fig 5** plots the influence of flux density on oxidation efficiency. Both CBZ and IBU were nearly totally
 293 degraded, with removal efficiencies higher than 90 % whatever the flux density applied. This confirms that
 294 contrary to the biodegradation process, photooxidation is non-selective [16,43]. **Fig. 5** shows that even a
 295 flux density as low as 4 W.m⁻² is enough to degrade the two molecules with removal efficiencies of 94 ± 2 %
 296 for CBZ and 92 ± 4 % for IBU. At 40 W.m⁻², these removal efficiencies increased to 99 ± 1 % for CBZ and
 297 98 ± 1 % for IBU. These only slight differences in removal efficiencies between 4 and 40 W.m⁻² show there
 298 is little interest in consuming 10 times more electricity to slightly better degrade the two micropollutants.
 299 These results show that the operating conditions and particularly HRT in the photoreactor were sufficient
 300 to degrade almost all the substances. In other words, even when flux density was low, the contact time
 301 was enough to degrade the target molecules. For this configuration, the contact time of around 6 hours
 302 was very long with regard to the experimental conditions applied. This finding is in agreement with the
 303 literature on photoreactors operating in batch mode showing very significant degradation of these two
 304 micropollutants [44] or other persistent compounds [19] after only a few hours of treatment.
 305 The removal efficiencies were similar and very high for both selected molecules—there was no preferential
 306 degradation of one molecule over the other. The difference, which in accordance with the literature is in
 307 favor of IBU [44], was not very significant here. Photodegradation experiments carried out on the
 308 compounds alone showed that IBU photodegraded more readily than CBZ (10 % – 20 % difference
 309 depending on the matrix) whereas the compounds in a cocktail were photodegraded at identical

310 efficiencies. These results confirm the non-selective nature of the photoreaction process, at least for the
 311 selected molecules. Note that the initial concentrations of CBZ and IBU were very different (IBU was 8
 312 times more concentrated than CBZ) yet their removal efficiencies were identical, which implies that the
 313 degradation rate was around 8 times higher for IBU than CBZ. However, given the non-selectivity of
 314 photodegradation, this result indicates that degradation rate was concentration-dependent and was
 315 almost proportional to the quantity of carbonaceous matter in the substances. In other words, it shows
 316 that the process degraded these two molecules indiscriminately and at the same removal efficiency.

317

318 **3.4. Coupling the membrane bioreactor with the photoreactor**

319 The photooxidation process was then associated with the MBR. Contrary to usual practice in the literature,
 320 this association was not in series where the oxidation process acts as a pre-treatment or post-treatment.
 321 The configuration proposed here, as illustrated in **Fig. 3**, positions the oxidation process on the MBR
 322 recirculation loop, so the oxidation step acts both as a post-treatment to degrade the biorecalcitrant
 323 molecules at the outlet of the MBR and as a pre-treatment that oxidizes these compounds to make them
 324 more biodegradable for the biological process.

325 Based on the results obtained for photooxidation alone (Section 3.3.), the lowest flux density of 4 W.m^{-2}
 326 was chosen as it assured the best removal-to-energy consumption trade-off. The flow rates of 7.5 L.d^{-1}
 327 were kept for both reactors (**Fig. 3**) in order to allow direct comparisons. The initial concentrations (C_{IN})
 328 were kept at $7 \mu\text{g.L}^{-1}$ for CBZ and $53 \mu\text{g.L}^{-1}$ for IBU.

329 To assess the efficiency of the coupling processes ($E_{\text{MBR+OX}}$) for micropollutant elimination, the all-round
 330 removal efficiency was calculated between the inlet (C_{IN}) and the outlet (C_{OUT}) at position ❶ of the global
 331 coupled system (**Fig. 3**), according to *Eq.1* as previously.

332 The effective degradation capacity of the two coupled processes was estimated using specific degradation
 333 rate ($r_{\text{MBR+OX}}$) based on the mass balance between the inlet and outlet of the overall system (**Fig. 3**):

$$334 \quad Q_{IN} \cdot C_{IN} = Q_{OUT} \cdot C_{OUT} + r_{\text{MBR+OX}} \cdot V_{\text{MBR+OX}} \cdot C_{TSS} \quad \text{eq.5}$$

$$335 \quad \text{with } V_{\text{MBR+OX}} = V_{\text{MBR}} + V_{\text{OX}}$$

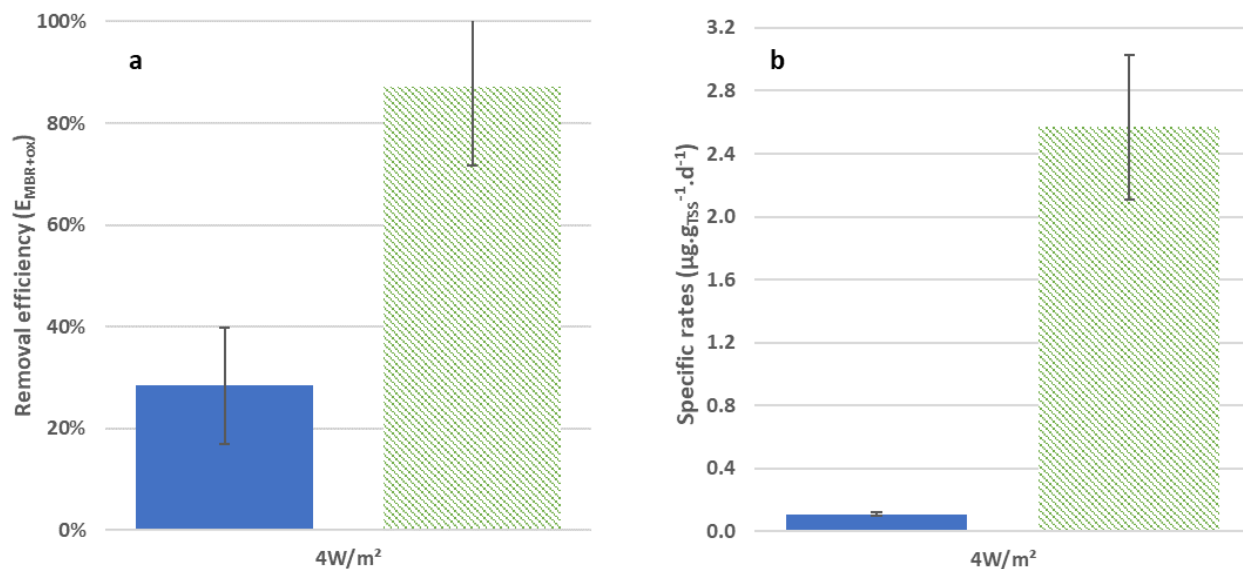
336 So, the specific degradation rate ($r_{\text{MBR+OX}}$) was:

$$337 \quad r_{\text{MBR+OX}} = \frac{Q_{IN} \cdot C_{IN} - (Q_{OUT} \cdot C_{OUT} + Q_S \cdot C_S)}{V_{\text{MBR+OX}} \cdot C_{TSS}} \quad \text{eq.6}$$

338 As $C_{OUT} = C_S$ at steady state and $Q_{OUT} + Q_S = Q_{IN}$, *eq.6* can be simplified as follows:

$$339 \quad r_{\text{MBR+OX}} = \frac{Q_{IN} \cdot (C_{IN} - C_{OUT})}{V_{\text{MBR+OX}} \cdot C_{TSS}} \quad \text{eq.7}$$

340



341
 342 **Figure 6:** carbamazepine [plain blue] and ibuprofen [green zebras] removal efficiencies (left) and specific rates (right)
 343 by the coupling of the membrane bioreactor with the photoreactor at 4W/m².

344
 345 The values for $E_{\text{MBR+OX}}$ and $r_{\text{MBR+OX}}$ are reported in **Fig. 6a** and **Fig. 6b**, respectively, for both IBU and CBZ. In
 346 this coupled configuration, CBZ was partially degraded ($E_{\text{MBR+OX}} = 28 \pm 11 \%$) and IBU was almost totally
 347 degraded ($E_{\text{MBR+OX}} = 87 \pm 15 \%$).

348 On the one hand and as expected, IBU was nearly totally degraded, as its removal reached $98 \pm 1 \%$ for
 349 MBR alone (**Fig. 4a**). Both removal efficiency and specific degradation rate were not significantly different
 350 between them. The slight decrease in degradation rate observed between the MBR alone ($r_{\text{MBR}} = 3.11$
 351 $\pm 0.04 \mu\text{g}\cdot\text{g}_{\text{TSS}}^{-1}\cdot\text{d}^{-1}$, **Fig. 4b**) and the coupled process ($r_{\text{MBR+OX}} = 2.57 \pm 0.46 \mu\text{g}\cdot\text{g}_{\text{TSS}}^{-1}\cdot\text{d}^{-1}$, **Fig. 6b**) can mainly
 352 be explained by the fact that the calculation for $r_{\text{MBR+OX}}$ considers the volumes of both reactors whereas
 353 the calculation of $r_{\text{MBRCoupled}}$ only considers the volume of the MBR. For this highly biodegradable
 354 compound, there was no positive or negative impact due to the oxidation process, which means that the
 355 experimental operating conditions for the coupled system in terms of residence time and microbial
 356 community were sufficient to degrade biodegradable substances.

357 On the other hand, CBZ is more persistent and thus poses a different challenge. Coupling the MBR with
 358 the photooxidation process allowed to improve the removal efficiency from less than 3 % for the MBR
 359 alone (**Fig. 4a**) to up to 28 % with the MBR coupled to the photoreactor (**Fig. 6a**). This improvement was
 360 expected, as the photoreactor alone had already shown a high removal efficiency of 94% (**Fig. 5**), in the
 361 tested oxidation conditions (flux density = $4 \text{ W}\cdot\text{m}^{-2}$, $\text{HRT}_{\text{OX}} = 6.4 \text{ h}$). Note, however, that these performances
 362 were achieved with a low-capacity oxidation process, as the HRT was 3.5 times longer in the MBR than in

363 the photoreactor. The specific degradation rate increased from $r_{\text{MBR}} = 0.01 \pm 0.12 \mu\text{g}\cdot\text{g}_{\text{TSS}}^{-1}\cdot\text{d}^{-1}$ with the MBR
364 alone (**Fig. 4b**) to $r_{\text{MBR+OX}} = 0.11 \pm 0.01 \mu\text{g}\cdot\text{g}_{\text{TSS}}^{-1}\cdot\text{d}^{-1}$ in the coupled-process configuration (**Fig. 6b**), which
365 means that the ratio between degradation rates of IBU and CBZ was increased by a factor 10. Coupling the
366 photoreactor to the MBR thus appears to increase the selective degradation of biorecalcitrant molecules.
367 It is difficult to compare our findings with published literature as there are almost no reports on coupling
368 an MBR with a photooxidation process. Only one study that described an integrated MBR with TiO_2
369 photocatalysis for wastewater treatment was found [45]. The authors showed up to 95% removal
370 efficiency for CBZ, but the initial CBZ concentration was very high ($10 \text{ mg}\cdot\text{L}^{-1}$) and so the final concentration
371 was always close to $1 \text{ mg}\cdot\text{L}^{-1}$. Moreover, their study was not operating in continuous mode but in
372 sequenced batch mode. Most other work in the literature proposes a combination of these two processes
373 associated in series.

374 The oxidation process positioned in pre-treatment seems to be effective for highly-concentrated effluents
375 [46, 47] and effluents containing mainly persistent compounds (pesticides, PAHs) [23,48]. Its utility lies in
376 the partial mineralization of the native molecules in order to make them biodegradable and consequently
377 eliminable by the biological process. However, the results are inconclusive for effluents with low
378 concentrations of micropollutants or effluents loaded with suspended solids. Indeed, these conditions not
379 only hinder irradiation of the catalysts but also inhibit the photodegradation process because the TSS
380 compete with the carbonaceous matter to be degraded [44].

381 Concerning the oxidation process positioned as a post-treatment, Leyva-Díaz et al. [24] showed that
382 removal performances were almost independent of type of AOP used (Fenton, H_2O_2 , photocatalysis). Work
383 on these associations (oxidation process as a post-treatment of a biological process) in continuous mode
384 amounts to a few dozen publications that mainly deal with low-concentration effluents. The studies tend
385 to show that the native molecules are partially affected but that the association has a strong impact on
386 toxicity [49] but also on biodegradability [22,25] and on the composition of process by-products. This
387 tendency was due to the non-selective nature of oxidative degradation technologies that indiscriminately
388 degrade all carbonaceous molecules. To complete the degradation of the by-products resulting from the
389 oxidative treatment, Leyva-Díaz et al. [24] proposed a combined MBR-POA-MBR configuration that allows
390 to reduce the toxicity of persistent native compounds by returning the oxidized effluent to a second
391 biological process.

392 These solutions involving additional treatments may be efficient but they are also expensive. A
393 recirculating combination, as proposed in this article, offers a compromise between pre-treatment and
394 post-treatment configurations without additional steps. It holds the advantages of post-treatment by

395 attacking the residual molecules of the biological treatment—which are by definition persistent—and thus
 396 allowing to complete degradation performance by returning the effluent made biodegradable back into
 397 the MBR. Experiments in the literature are generally conducted with mature energy-intensive processes
 398 (ozonation [25], fenton [22]) or by oversized homogeneous or heterogeneous photocatalysis (high
 399 irradiation conditions for small volumes, or very long residence times [50]. Under these conditions, they
 400 can non-selectively increase the removal rates by several dozen percent COD or BOD [22,25]. However,
 401 they still do not preferentially target persistent compounds, which makes the system less efficient (high
 402 cost or oversized) for removing specific POPs.

403
 404 **3.5. Intensification of membrane bioreactor performance: synergic effect of the photoreactor**

405 To highlight any potential synergy enabled by the proposed coupling, removal efficiency ($E_{MBRCoupled}$) and
 406 specific degradation rate ($r_{MBRCoupled}$) were estimated for the MBR alone but operating within the overall
 407 system, i.e. coupled with the photoreactor, in order to compare the results against the values obtained for
 408 the MBR alone (eq.1 and eq.2) and the coupling process (eq.1 and eq.7).

409 Removal efficiency ($E_{MBRCoupled}$) was calculated as follows:

410
$$E_{MBRCoupled} = \frac{C_{IN} + C_{OX} - C_{OUT}}{C_{IN} + C_{OX}} \cdot 100 \quad eq.8$$

411 The calculation of $r_{MBRCoupled}$, i.e. the specific rate of the MBR intensified by the oxidation process, was
 412 based on mass balance between the inlets (Q_{IN} and Q_{OX} , Fig. 3) and the outlets (Q_{OUT} and Q_{OX} , Fig. 3) of the
 413 MBR. The capacity of the coupled MBR was defined as the volume of the MBR alone (V_{MBR}), leading to the
 414 following equation:

415
$$Q_{IN} \cdot C_{IN} + Q_{OX} \cdot C_{OXout} = Q_{OX} \cdot C_{OXin} + (Q_S + Q_{OUT}) \cdot C_{OUT} + r_{MBRCoupled} \cdot V_{MBR} \cdot C_{TSS} \quad eq.9$$

416 Then:

417
$$r_{MBRCoupled} = \frac{Q_{IN} \cdot C_{IN} + Q_{OX} \cdot C_{OXout} - Q_{OX} \cdot C_{OXin} - (Q_{OUT} + Q_S) \cdot C_{OUT}}{V_{MBR} \cdot C_{TSS}} \quad eq.10$$

418 and:

419
$$r_{MBRCoupled} = \frac{Q_{IN} \cdot (C_{IN} + C_{OXout} - 2 \cdot C_{OUT})}{V_{MBR} \cdot C_{TSS}} \quad eq.11$$

420 **Table 2:** Efficiency and removal rates of both pharmaceuticals for the different systems.

	Compound	MBR alone	MBR coupled	MBR+OX
Efficiency (%)	CBZ	2.7 ± 28.7	58.9 ± 6.6	28.3 ± 11.5
	IBU	97.9 ± 1.3	89.5 ± 12.7	87.2 ± 15.5
Specific rate (µg·g_{TSS}⁻¹·d⁻¹)	CBZ	0.01 ± 0.12	0.13 ± 0.05	0.11 ± 0.01
	IBU	3.11 ± 0.04	3.01 ± 0.49	2.57 ± 0.46

422 **Table 2** reports the removal efficiencies and specific rates for both IBU and CBZ in the three configurations,
423 i.e. MBR alone (MBR), MBR alone in the coupling system (MBR Coupled), and the global coupled system
424 (MBR+OX).

425 For IBU, the specific degradation rate of the MBR in the coupled process is not vastly different from the
426 specific degradation rate of the MBR alone or the global coupled system. As stated previously, IBU is
427 already highly biodegradable and so the photooxidation process did not significantly improve IBU removal.

428 For CBZ, specific degradation rate went from $0.01 \pm 0.12 \mu\text{g}\cdot\text{g}_{\text{TSS}}^{-1}\cdot\text{d}^{-1}$ for the MBR alone to $0.13 \pm$
429 $0.05 \mu\text{g}\cdot\text{g}_{\text{TSS}}^{-1}\cdot\text{d}^{-1}$ for the MBR in the coupled system (MBR_{Coupled}) (**Table 2**). This finding shows that MBR
430 performance on degrading CBZ was improved by the insertion of the oxidation process. Plugging the
431 oxidation process into the MBR thus appears to intensify the degradation capacity selectively towards
432 refractory molecules. Thus, while the ratio of degradation rates between IBU and CBZ was 300 for MBR
433 alone, it tended towards 30 when the two processes were coupled (**Table 2**).

434 Let's address the relevance of this type of coupling (a configuration with recirculation in the photoreactor)
435 compared to an association in series either in pre-treatment or post-treatment. The value of the oxidation
436 process is that it can degrade refractory compounds, knowing that biodegradable carbonaceous
437 compounds are currently perfectly well managed by biological processes. The results reported in **Table 2**
438 show that IBU, which is a readily biodegradable compound, was almost totally degraded under the
439 conditions set by the biological process (degradation rate remained stable whatever the MBR
440 configuration: alone or coupled). The oxidation process therefore had a secondary role, neither improving
441 nor disrupting the degradation of IBU. For CBZ, specific degradation rate was very sensitive to
442 configuration. These results reflect the fact that this association intensified the degradation of the
443 refractory compound. In a way, as the rate of IBU degradation was stable, the oxidation process acted
444 selectively by privileging the degradation of CBZ. This behavior is assignable to the configuration that
445 consisted in plugging the photoreactor in recirculation mode on the MBR. Indeed, by allowing the effluent
446 and thus the compounds to circulate within the system, each process acted in a complementary way by
447 playing its specific function. The MBR largely degraded the biodegradable compounds, leaving a minority
448 to flow into the oxidation process, whereas the refractory compounds passing through the MBR flowed
449 into the oxidation process. The selection induced between refractory and biodegradable compounds
450 modifies the composition of the effluent, which was artificially concentrated in refractory compounds.

451 In the literature, associations in-series have proven effective, enabling high degradation rates. On the one
452 hand, these associations can be costly and require the development of over-scaled oxidation processes
453 that need to operate under the same conditions as the MBR (flow rate, residence time, TSS management).

454 On the other hand, the main but rare results obtained on coupled systems (in continuous mode) show
455 high degradation rates on global performance indicators such as COD, BOD, and toxicity. However, these
456 associations do not promote the degradation of the refractory compounds targeted under EU regulations
457 [2]. They deliver a non-selective 'all-round' degradation of pollutant load that makes them under-efficient
458 for the target substances, i.e. cost increase, oversizing, and overestimated operating conditions. The
459 system proposed here works differently by proposing to exploit on the advantages of each of the two
460 processes involved. By recirculating the effluent within the two processes, the system intensifies the
461 capacities of each process by selecting the compounds requiring further treatment.
462 For future tests, this configuration will enable analysts to dissociate the roles on feed and recirculation
463 flows, which is not possible with in-series configurations. For example, if the recirculation flow rate (Q_{OX})
464 is increased while keeping the residence time identical within each process ($Q_{IN} = \text{constant}$, V_{MBR} and V_{OX}
465 constant), the number of times the effluent passes through the oxidation process will increase
466 proportionally to this flow rate (Q_{OX}): by applying $Q_{OX} = n \cdot Q_{IN}$. It is anticipated that these operating
467 conditions could be favorable to transform the compounds into by-products that may potentially become
468 more biodegradable than the native molecules.

469

470 **4. Conclusion**

471 An innovative continuous process coupling a membrane bioreactor and a photoreactor is proposed for the
472 removal of two pharmaceuticals (ibuprofen and carbamazepine) from wastewater. Implementing the
473 photooxidation process in a recirculation loop on the membrane bioreactor had no negative impact on the
474 removal efficiency of carbon, nitrogen and phosphorus pollution. No negative impact on the removal
475 efficiency of biodegradable compounds such as ibuprofen was found, while at the same time a 10-fold
476 improvement in the removal efficiency of biorecalcitrant compounds such as carbamazepine occurred.
477 Furthermore, these results were achieved with a very low flux density of just 4 W.m^{-2} .

478 The interest and potential of this configuration coupling a photoreactor to the recirculation loop of
479 the bioreactor have been discussed. The results reveal the relevance of this association which must
480 be studied and optimized in order to intensify the performance of the system. The purpose is to get
481 rid of the constraints imposed by the series configuration, by proposing to partially treat the micro
482 pollutants during their passage in the oxidation process. Then, the by-products of the oxidized
483 pollutants can be biodegraded by the membrane bioreactor. In this sense and contrary to the
484 associations of reactors in series, this configuration makes it possible to play on the respective

485 residence times of two reactors, by varying the volumes of the reactors, but especially, the number
486 of passages in the photo-reactor, by modulating the recirculation flow. These conditions should
487 make it possible to intensify the performance of the coupling and in particular to accentuate the
488 elimination of the by-products resulting from the degradation of the parent substances. In the long
489 term, the bioreactor should also be associated with a solar photoreactor in order to take into account
490 the effects of discontinuities in the solar resource (day/night cycle, cloudy periods) on the treatment
491 capacities of the photoreactor and consequently of the coupled system.

492

493 **Acknowledgment**

494 This work received European sponsorship via the FEDER funds under the “Interreg SUDOE” program
495 (Innovéc’eau SOE1/P1/F0173) as well as regional sponsorship (PHOTODEPOL, N°19015248). This work was
496 supported by French “Investments for the future” (“Investissements d’Avenir”) program managed by the
497 National Agency for Research (ANR) under contract ANR-10-LABX-22-01 (labex SOLSTICE).

498

499 **References**

- 500 [1] European Parliament, DCE 2013/39/EU, Official Journal of European Union, European Union,
501 2013. Official Journal of European Union.
- 502 [2] European Commission, Directive 2000/60/EC of the European Parliament and of the Council of 23
503 October 2000, establishing a framework for community action in the field of water policy, Off. J.
504 Eur. Union. (2000) 1–73. <http://eur-lex.europa.eu/eli/dir/2000/60/oj>.
- 505 [3] KNAPPE, Knowledge and Need Assessment on Pharmaceutical Product in Environmental waters,
506 6th framework research program of the European Commission (2007-2010), in: 2007.
- 507 [4] W.C. Li, Occurrence, sources, and fate of pharmaceuticals in aquatic environment and soil,
508 Environ. Pollut. 187 (2014) 193–201. <https://doi.org/10.1016/j.envpol.2014.01.015>.
- 509 [5] B. Petrie, R. Barden, B. Kasprzyk-Hordern, A review on emerging contaminants in wastewaters
510 and the environment: Current knowledge, understudied areas and recommendations for future
511 monitoring, Water Res. 72 (2015) 3–27. <https://doi.org/10.1016/j.watres.2014.08.053>.
- 512 [6] B. Reoyo-Prats, D. Aubert, C. Menniti, W. Ludwig, J. Sola, M. Pujo-Pay, P. Conan, O. Verneau, C.
513 Palacios, Multicontamination phenomena occur more often than expected in Mediterranean
514 coastal watercourses: Study case of the Têt River (France), Sci. Total Environ. (2017).
515 <https://doi.org/10.1016/j.scitotenv.2016.11.019>.

- 516 [7] S. Lacorte, S. Luis, C. Gómez-Canela, T. Sala-Comorera, A. Courtier, B. Roig, A.M. Oliveira-Brett, C.
517 Joannis-Cassan, J.I. Aragonés, L. Poggio, T. Noguer, L. Lima, C. Barata, C. Calas-Blanchard,
518 Pharmaceuticals released from senior residences: occurrence and risk evaluation, *Environ. Sci.*
519 *Pollut. Res.* 25 (2018) 6095–6106. <https://doi.org/10.1007/s11356-017-9755-1>.
- 520 [8] B. Reoyo-Prats, D. Aubert, A. Sellier, B. Roig, C. Palacios, Dynamics and sources of
521 pharmaceutically active compounds in a coastal Mediterranean river during heavy rains, *Environ.*
522 *Sci. Pollut. Res.* (2017). <https://doi.org/10.1007/s11356-017-0880-7>.
- 523 [9] P. Gao, Y. Ding, H. Li, I. Xagorarakis, Occurrence of pharmaceuticals in a municipal wastewater
524 treatment plant: Mass balance and removal processes, *Chemosphere.* 88 (2012) 17–24.
525 <https://doi.org/10.1016/j.chemosphere.2012.02.017>.
- 526 [10] S.J. Kimosop, Z.M. Getenga, F. Orata, V.A. Okello, J.K. Cheruiyot, Residue levels and discharge
527 loads of antibiotics in wastewater treatment plants (WWTPs), hospital lagoons, and rivers within
528 Lake Victoria Basin, Kenya, *Environ. Monit. Assess.* 188 (2016) 90100.
529 <https://doi.org/10.1007/s10661-016-5534-6>.
- 530 [11] P. Verlicchi, A. Galletti, M. Petrovic, D. BarcelÓ, Hospital effluents as a source of emerging
531 pollutants: An overview of micropollutants and sustainable treatment options, *J. Hydrol.* 389
532 (2010) 416–428. <https://doi.org/10.1016/j.jhydrol.2010.06.005>.
- 533 [12] C. Laurencé, M. Rivard, T. Martens, C. Morin, D. Buisson, S. Bourcier, M. Sablier, M.A. Oturan,
534 Anticipating the fate and impact of organic environmental contaminants: A new approach applied
535 to the pharmaceutical furosemide, *Chemosphere.* 113 (2014) 193–199.
536 <https://doi.org/10.1016/j.chemosphere.2014.05.036>.
- 537 [13] M. Clara, B. Strenn, O. Gans, E. Martinez, N. Kreuzinger, H. Kroiss, Removal of selected
538 pharmaceuticals, fragrances and endocrine disrupting compounds in a membrane bioreactor and
539 conventional wastewater treatment plants, *Water Res.* 39 (2005) 4797–4807.
540 <https://doi.org/10.1016/j.watres.2005.09.015>.
- 541 [14] J.M.J. Millanar-Marfa, L. Borea, S.W. Hasan, M.D.G. de Luna, V. Belgiorno, V. Naddeo, Advanced
542 membrane bioreactors for emerging contaminant removal and quorum sensing control, Elsevier
543 B.V., 2020. <https://doi.org/10.1016/B978-0-12-819854-4.00006-X>.
- 544 [15] M. Brienza, M. Mahdi Ahmed, A. Escande, G. Plantard, L. Scrano, S. Chiron, S.A. Bufo, V. Goetz,
545 Use of solar advanced oxidation processes for wastewater treatment: Follow-up on degradation
546 products, acute toxicity, genotoxicity and estrogenicity, *Chemosphere.* 148 (2016) 473–480.
547 <https://doi.org/10.1016/j.chemosphere.2016.01.070>.

- 548 [16] S. Malato, J. Blanco, A. Vidal, D. Alarcón, M.I. Maldonado, J. Cáceres, W. Gernjak, Applied studies
549 in solar photocatalytic detoxification: An overview, *Sol. Energy*. 75 (2003) 329–336.
550 <https://doi.org/10.1016/j.solener.2003.07.017>.
- 551 [17] J. Blanco, S. Malato, *Solar detoxification*, UNESCO, 2003.
- 552 [18] J.M. Herrmann, Heterogeneous photocatalysis: State of the art and present applications, *Top.*
553 *Catal.* 34 (2005) 49–65. <https://doi.org/10.1007/s11244-005-3788-2>.
- 554 [19] M. Brienza, M. Mahdi Ahmed, A. Escande, G. Plantard, L. Scrano, S. Chiron, S. A. Bufo, V. Goetz,
555 Relevance of a photo-Fenton like technology based on peroxymonosulphate for 17 β -estradiol
556 removal from wastewater, *Chem. Eng. J.* 257 (2014) 191–199.
557 <https://doi.org/10.1016/j.cej.2014.07.061>.
- 558 [20] I. Oller, S. Malato, J.A. Sánchez-Pérez, Combination of Advanced Oxidation Processes and
559 biological treatments for wastewater decontamination-A review, *Sci. Total Environ.* 409 (2011)
560 4141–4166. <https://doi.org/10.1016/j.scitotenv.2010.08.061>.
- 561 [21] H. Monteil, Y. Péchaud, N. Oturan, M.A. Oturan, A review on efficiency and cost effectiveness of
562 electro- and bio-electro-Fenton processes: Application to the treatment of pharmaceutical
563 pollutants in water, *Chem. Eng. J.* 376 (2019). <https://doi.org/10.1016/j.cej.2018.07.179>.
- 564 [22] S. Chen, D. Sun, J.S. Chung, Treatment of pesticide wastewater by moving-bed biofilm reactor
565 combined with Fenton-coagulation pretreatment, *J. Hazard. Mater.* 144 (2007) 577–584.
566 <https://doi.org/10.1016/j.jhazmat.2006.10.075>.
- 567 [23] V. Sarria, S. Parra, N. Adler, P. Péringer, N. Benitez, C. Pulgarin, Recent developments in the
568 coupling of photoassisted and aerobic biological processes for the treatment of biorecalcitrant
569 compounds, *Catal. Today.* 76 (2002) 301–315. [https://doi.org/10.1016/S0920-5861\(02\)00228-6](https://doi.org/10.1016/S0920-5861(02)00228-6).
- 570 [24] J.C. Leyva-Díaz, C. López-López, J. Martín-Pascual, M.M. Muñío, J.M. Poyatos, Kinetic study of the
571 combined processes of a membrane bioreactor and a hybrid moving bed biofilm reactor-
572 membrane bioreactor with advanced oxidation processes as a post-treatment stage for
573 wastewater treatment, *Chem. Eng. Process. Process Intensif.* 91 (2015) 57–66.
574 <https://doi.org/10.1016/j.cep.2015.03.017>.
- 575 [25] A.M. Chávez, O. Gimeno, A. Rey, G. Pliego, A.L. Oropesa, P.M. Álvarez, F.J. Beltrán, Treatment of
576 highly polluted industrial wastewater by means of sequential aerobic biological oxidation-ozone
577 based AOPs, *Chem. Eng. J.* 361 (2019) 89–98. <https://doi.org/10.1016/j.cej.2018.12.064>.
- 578 [26] C. Joannis-Cassan, A.S. Rodriguez Castillo, C. Dezani, C. Gómez-Canela, B. Reoyo-Prats, C. Calas-
579 Blanchard, C. Barata, S. Lacorte, G. Plantard, Towards an innovative combined process coupling

580 biodegradation and photo-oxidation for the removal of pharmaceutical residues, *J. Chem.*
581 *Technol. Biotechnol.* 96 (2021) 755–763. <https://doi.org/10.1002/jctb.6589>.

582 [27] V. Osorio, A. Larrañaga, J. Aceña, S. Pérez, D. Barceló, Concentration and risk of pharmaceuticals
583 in freshwater systems are related to the population density and the livestock units in Iberian
584 Rivers, *Sci. Total Environ.* 540 (2015) 267–277. <https://doi.org/10.1016/j.scitotenv.2015.06.143>.

585 [28] A.M.P.T. Pereira, L.J.G. Silva, C.S.M. Laranjeiro, L.M. Meisel, C.M. Lino, A. Pena, Science of the
586 Total Environment Human pharmaceuticals in Portuguese rivers : The impact of water scarcity in
587 the environmental risk, *Sci. Total Environ.* 609 (2017) 1182–1191.
588 <https://doi.org/10.1016/j.scitotenv.2017.07.200>.

589 [29] E. Van Den Brandhof, M. Montforts, Ecotoxicology and Environmental Safety Fish embryo toxicity
590 of carbamazepine , diclofenac and metoprolol, *Ecotoxicol. Environ. Saf.* 73 (2010) 1862–1866.
591 <https://doi.org/10.1016/j.ecoenv.2010.08.031>.

592 [30] L.H. Heckmann, A. Callaghan, H.L. Hooper, R. Connon, T.H. Hutchinson, S.J. Maund, R.M. Sibly,
593 Chronic toxicity of ibuprofen to *Daphnia magna*: Effects on life history traits and population
594 dynamics, *Toxicol. Lett.* 172 (2007) 137–145. <https://doi.org/10.1016/j.toxlet.2007.06.001>.

595 [31] D. Kanakaraju, B.D. Glass, M. Oelgemöller, Titanium dioxide photocatalysis for pharmaceutical
596 wastewater treatment, *Environ. Chem. Lett.* 12 (2014) 27–47. [https://doi.org/10.1007/s10311-](https://doi.org/10.1007/s10311-013-0428-0)
597 [013-0428-0](https://doi.org/10.1007/s10311-013-0428-0).

598 [32] OECD Guideline for the Testing of Chemicals, Simulation Test - Aerobic Sewage Treatment,
599 Organisation for economic co-operation and development, Paris, 2001.
600 [doi:10.1787/9789264067394](https://doi.org/10.1787/9789264067394)

601 [33] J. Seira, C. Sablayrolles, M. Montréjaud-Vignoles, C. Albasi, C. Joannis-Cassan, Elimination of an
602 anticancer drug (cyclophosphamide) by a membrane bioreactor: Comprehensive study of
603 mechanisms, *Biochem. Eng. J.* 114 (2016) 155–163. <https://doi.org/10.1016/j.bej.2016.07.001>.

604 [34] N. Han Tran, M. Reinhard, K. Yew-hoong Gin, Occurrence and fate of emerging contaminants in
605 municipal wastewater treatment plants from different geographical regions-a review, *Water Res.*
606 133 (2018) 182–207. <https://doi.org/10.1016/j.watres.2017.12.029>.

607 [35] O.M. Rodriguez-Narvaez, J.M. Peralta-Hernandez, A. Goonetilleke, E.R. Bandala, Treatment
608 technologies for emerging contaminants in water: A review, *Chem. Eng. J.* 323 (2017) 361–380.
609 <https://doi.org/10.1016/j.cej.2017.04.106>.

610 [36] G. Plantard, T. Janin, V. Goetz, S. Brosillon, Solar photocatalysis treatment of phytosanitary
611 refuses: Efficiency of industrial photocatalysts, *Appl. Catal. B Environ.* 115–116 (2012) 38–44.
612 <https://doi.org/10.1016/j.apcatb.2011.11.034>.

- 613 [37] American Public Health Association, American Water Works Association, Water Environment
614 Federation, Standard methods for the examination of water and wastewater, Washington D.C,
615 2005.
- 616 [38] N. Tadkaew, F.I. Hai, J.A. McDonald, S.J. Khan, L.D. Nghiem, Removal of trace organics by MBR
617 treatment: The role of molecular properties, *Water Res.* 45 (2011) 2439–2451.
618 <https://doi.org/10.1016/j.watres.2011.01.023>.
- 619 [39] M. Kim, P. Guerra, A. Shah, M. Parsa, M. Alaei, S.A. Smyth, Removal of pharmaceuticals and
620 personal care products in a membrane bioreactor wastewater treatment plant, *Water Sci.*
621 *Technol.* 69 (2014) 2221–2229. <https://doi.org/10.2166/wst.2014.145>.
- 622 [40] F. Çeçen, G. Gül, Biodegradation of five pharmaceuticals: estimation by predictive models and
623 comparison with activated sludge data, *Int. J. Environ. Sci. Technol.* 18 (2021) 327–340.
624 <https://doi.org/10.1007/s13762-020-02820-y>.
- 625 [41] P. Verlicchi, M. Al Aukidy, E. Zambello, Occurrence of pharmaceutical compounds in urban
626 wastewater: Removal, mass load and environmental risk after a secondary treatment-A review,
627 *Sci. Total Environ.* 429 (2012) 123–155. <https://doi.org/10.1016/j.scitotenv.2012.04.028>.
- 628 [42] S. Suarez, J.M. Lema, F. Omil, Removal of Pharmaceutical and Personal Care Products (PPCPs)
629 under nitrifying and denitrifying conditions, *Water Res.* 44 (2010) 3214–3224.
630 <https://doi.org/10.1016/j.watres.2010.02.040>.
- 631 [43] D. Kanakaraju, B.D. Glass, M. Oelgemöller, Advanced oxidation process-mediated removal of
632 pharmaceuticals from water: A review, *J. Environ. Manage.* 219 (2018) 189–207.
633 <https://doi.org/10.1016/j.jenvman.2018.04.103>.
- 634 [44] B. Reoyo-Prats, C. Joannis-Cassan, M. Hammadi, V. Goetz, C. Calas-blanchard, G. Plantard, Photo-
635 oxidation of three major pharmaceuticals in urban wastewater under artificial and solar
636 irradiations., *J. Photochemistry Photobiol. A Chem.* (2021).
- 637 [45] G. Laera, M.N. Chong, B. Jin, A. Lopez, An integrated MBR-TiO₂ photocatalysis process for the
638 removal of Carbamazepine from simulated pharmaceutical industrial effluent, *Bioresour. Technol.*
639 102 (2011) 7012–7015. <https://doi.org/10.1016/j.biortech.2011.04.056>.
- 640 [46] I. Oller, S. Malato, J.A. Sánchez-Pérez, M.I. Maldonado, R. Gassó, Detoxification of wastewater
641 containing five common pesticides by solar AOPs-biological coupled system, *Catal. Today.* 129
642 (2007) 69–78. <https://doi.org/10.1016/j.cattod.2007.06.055>.
- 643 [47] H. Wu, S. Wang, H. Kong, T. Liu, M. Xia, Performance of combined process of anoxic baffled
644 reactor-biological contact oxidation treating printing and dyeing wastewater, *Bioresour. Technol.*

- 645 98 (2007) 1501–1504. <https://doi.org/10.1016/j.biortech.2006.05.037>.
- 646 [48] M.D. Marsolek, M.J. Kirisits, K.A. Gray, B.E. Rittmann, Coupled photocatalytic-biodegradation of
647 2,4,5-trichlorophenol: Effects of photolytic and photocatalytic effluent composition on bioreactor
648 process performance, community diversity, and resistance and resilience to perturbation, *Water*
649 *Res.* 50 (2014) 59–69. <https://doi.org/10.1016/j.watres.2013.11.043>.
- 650 [49] B.M. Esteves, C.S.D. Rodrigues, R.A.R. Boaventura, F.J. Maldonado-Hódar, L.M. Madeira, Coupling
651 of acrylic dyeing wastewater treatment by heterogeneous Fenton oxidation in a continuous
652 stirred tank reactor with biological degradation in a sequential batch reactor, *J. Environ. Manage.*
653 166 (2016) 193–203. <https://doi.org/10.1016/j.jenvman.2015.10.008>.
- 654 [50] A. Dixit, A.J. Tirpude, A.K. Mungray, M. Chakraborty, Degradation of 2, 4 DCP by sequential
655 biological-advanced oxidation process using UASB and UV/TiO₂/H₂O₂, *Desalination.* 272 (2011)
656 265–269. <https://doi.org/10.1016/j.desal.2011.01.035>.